Pergamon

PII: S0306-4522(97)00583-6

Neuroscience Vol. 84, No. 4, pp. 1163–1175, 1998
Copyright © 1998 IBRO. Published by Elsevier Science Ltd
Printed in Great Britain. All rights reserved
0306-4522/98 $19.00+0.00

POSTNATAL DEVELOPMENT OF EXCITATORY SYNAPTIC INPUT TO THE RAT NEOSTRIATUM: AN ELECTRON MICROSCOPIC STUDY

N. A. SHARPE and J. M. TEPPER*

Aidekman Research Center, Center for Molecular and Behavioral Neuroscience and Program In Cellular and Molecular Biodynamics, Rutgers, The State University of New Jersey, Newark, New Jersey, U.S.A.

Abstract—The distribution and density of asymmetric synapses including biocytin-labelled corticostriatal synapses of the rat neostriatum were examined at postnatal day 10 (P10), P15, P21 and in adults. The density of asymmetric synapses in the adult neostriatum (28.0 synapses/100 μm^2) was significantly greater than that in neonates at P15 (14.4 synapses/100 μm^2) and P10 (11.5 synapses/100 μm^2), but not at P21 (24.2 ± 1.5 synapses/100 μm^2). The increased density of asymmetric synapses in the adult neostriatum was due primarily to an increase in the number of axospinous synapses. The density of axospinous synapses was greatest in adults (22.3 synapses/100 μm^2) and significantly less at P21 (15.3 synapses/100 μm^2), P15 (5.9 synapses/100 μm^2), and P10 (2.0 synapses/100 μm^2). The density of axodendritic synapses, however, remained similar at all ages (adult, 3.9 ± 1.1 synapses/100 μm^2; P21, 6.0 ± 1.2 synapses/100 μm^2; P15, 5.7 ± 0.8 synapses/100 μm^2 or P10, 7.2 ± 1.3 synapses/100 μm^2). Iontophoretic injection of biocytin into the lateral frontal agranular cortex produced labelling of corticostriatal afferents which formed asymmetric synapses in the neostriatum. The distribution of termination sites of biocytin-labelled corticostriatal boutons showed a pattern of development similar to the unlabelled asymmetric synapses.

The present study shows that the increase in the overall number of asymmetric synapses over the first three postnatal weeks can be attributed to an increase in the density of asymmetric axospinous synapses. During the same period little change is noted in the number or density of asymmetric axodendritic synapses. These changes in excitatory synaptic input to medium spiny neurons may explain some of the previously described electrophysiological differences noted between the neonatal and adult neostriatum.
© 1998 IBRO. Published by Elsevier Science Ltd.

Key words: basal ganglia, biocytin, dendritic spine, development, neonatal, corticostriatal.

The majority of afferents to the basal ganglia terminate in the neostriatum. Various areas of the neocortex, including the prefrontal, motor, somatosensory and visual areas, along with the thalamus, form the primary excitatory inputs to the dorsal neostriatum.[15,17,23b,28,39,41] The majority of cortical afferents in the adult neostriatum form asymmetric synapses onto spine heads.[17,25,26,28,41] Thalamic afferents terminate onto both spine heads and dendritic shafts.[17,25,26,38] Both of these afferents are believed to be excitatory and use glutamate or another excitatory amino acid as their neurotransmitter.[6] The anatomy and electrophysiology of cortical input to the neostriatum of the adult rat have been studied extensively.[6,10,17,24,37,46,51] The morphological and electrophysiological properties of the medium spiny neuron, the principal neuron of the neostriatum, have also been well characterized in the adult rat.[5,16,18,53] Information is available on the postnatal development of feline and primate neostriatum.[1,7,12,15,21,30] However, only limited information is available on the postnatal development of the corticostriatal pathway[19] and other afferents to the rat neostriatal medium spiny neuron.[22,43–45]

Light microscopic studies have shown that the dendritic morphology of the adult and neonatal medium spiny neuron differ significantly in felines, primates and rats with the density of dendritic spines increasing over development.[1,12,21,43–45] In the adult rat, the medium spiny neuron is highly spiny, with a maximum spine density of 4–6 spines/μm of dendrite measured approximately 80 μm from the soma.[52] In the early neonatal rat, the medium spiny neuron is almost totally aspiny, and possesses thin and varicose dendrites.[45] The greatest increase in spine density occurs during the third postnatal week, corresponding to the time when the majority of the cortical and thalamic afferents innervate the neostriatum.[19] This timing also corresponds to the period when the most significant electrophysiological changes are noted.[34,43,44]

Characterization of corticostriatal and other excitatory synaptic inputs to the medium spiny neuron over postnatal development may provide a basis for explaining functional differences between

*To whom correspondence should be addressed.

Abbreviations: DAB, 3,3′-diaminobenzidine; EPSP, excitatory postsynaptic potential; IPSP, inhibitory postsynaptic potential; P, postnatal day; PB, phosphate buffer.

the developing neonatal and adult neostriatum and medium spiny neuron.[33,34,39,41,43,44] Although it has been suggested, on electrophysiological grounds, that the cortex does innervate the neonatal neostriatum,[33,43,44] the synaptic organization and postsynaptic targets of corticostriatal and other excitatory afferents in neonates are not known.

The present study examines the morphology and distribution of asymmetric synapses, including biocytin-labelled cortical afferents over postnatal development in the rat neostriatum. Portions of this work have been presented in abstract form.[39,41]

EXPERIMENTAL PROCEDURES

Animals and tract tracing

Adult (greater than eight weeks-of-age), postnatal day 21 (P21; with P1 defined as the day of birth), P14/15 (P15) and P9/10 (P10) Sprague–Dawley rats, supplied from either the Institute of Animal Behavior, Rutgers, The State University of NJ, Newark, NJ; or Charles River Laboratories, Kingston, NY, were used for all experiments. For each group, pups were obtained from three to four litters with at least one pup from each litter. Five adults were utilized for the experimental procedures. All animals were treated in strict accordance with guidelines set forth in the PHS manual, "Guide for the Care and Use of Laboratory Animals".

Rats were anaesthetized with ketamine (Research Biochemicals International [RBI], Natick, MA; 80 mg/kg) and xylazine (RBI, Natick, MA; 15 mg/kg) in 0.9% saline administered intraperitoneally. Since ear bars could not be used in neonates younger than P21, the pups were installed in the stereotaxic apparatus by taping the snout (while not blocking the airways) and caudal skull to a small stage seated in the stereotaxic apparatus. Glass micropipettes were pulled from 2 mm capillary tubing (World Precision Inc., Sarasota, FL) on a vertical pipette puller (Narishige Scientific, Tokyo, Japan). The tips were broken back to approximately 50 μm under microscopic control and micropipettes filled with 3–5% biocytin (Sigma, St Louis, MO) in 1 M potassium acetate. Micropipettes were lowered into the ipsilateral lateral frontal agranular cortex and biocytin was iontophoretically injected (7.5 μA, 7 s pulse, 50% duty cycle, for 15 min in the neonates and for 40 min in adults). Stereotaxic coordinates in adults were from Bregma: anterior +2.5 mm, lateral 3.4 mm, ventral 1.75 mm from cortical surface.[35] Coordinates were empirically adjusted in neonates to obtain similar injection locations in both adults and neonates and ranged from anterior +2.3 to 2.6 mm, lateral 2.0–2.2 mm, ventral 1.8–2.3 mm.

Tissue processing

Four to 24 h post-injection (time was age-dependent; the older the animal the longer the post-injection time), rats were given an overdose of urethane (Sigma, St Louis, MO), perfused with 10–40 ml oxygenated Ringer's followed by 100–400 ml of a 4% paraformaldehyde–0.8% glutaraldehyde solution (pH 7.2) and the brain excised. The brains were blocked and postfixed in the aldehyde fixative solution for at least 24 h. Parasagittal sections (30–60 μm) containing neostriatum and the cortical injection site were obtained using a Vibratome. Sections were processed for sequential light and electron microscopy. The sections were rinsed in 0.15 M phosphate buffer (PB) and pre-incubated for 5 min in 0.1 M glycine followed by 5 min in 0.5% hydrogen peroxide in PB. To increase antibody penetration without critically compromising the ultrastructural preservation, sections were incubated with 0.01% Triton (Electron Microscopy Sciences, Ft Washington, PA.) in PB for 30 (P10) or 60 (P15 and P21) min depending on age. The Triton incubation was omitted in adults. Following multiple PB washes, sections were incubated in an avidin–biotin–peroxidase complex (Vector Labs, Burlingame, CA; 1:100 in PB) for 24 h (room temperature or 4°C). After further washes with PB, biocytin labelling was visualized by incubating in 0.05% 3,3′-diaminobenzidine (DAB; Electron Microscopy Sciences, Ft Washington, PA) containing 0.03% hydrogen peroxide for 15–20 min. Sections were postfixed in 1% osmium tetroxide for 60 min, followed by multiple PB washes. Sections were dehydrated in an ascending series of ethanol, and stained *en bloc* with 1% uranyl acetate for 60 min. Sections were infiltrated overnight with Durcupan® ACM (Fluka), were placed between liquid release coated slides and coverslips and cured at 60°C for 24–48 h.

Analysis

Tissue was initially evaluated at the light microscopic level. Areas of biocytin labelling in the dorsal lateral neostriatum and the injection sites in the cortex were identified and photographed. Coverslips were then removed and areas of interest in the dorsal lateral neostriatum were trimmed out and mounted onto Polybed 812® blocks using cyanoacrylate glue. Ultrathin sections (50–80 nm) were obtained using an American Optical Ultramicrotome and collected on Formvar-coated slotted or 200 mesh grids. Sections were stained with lead citrate (0.5%) and examined using a Phillips CM10 transmission electron microscope at 80 kV. Only synapses forming asymmetric membrane specializations were analysed.

The density of asymmetric synapses was determined by analysing randomly photographed electron micrographs taken at a magnification of 21,000×. Sections from which electron micrographs were obtain were selected randomly via a computer generated random number table per animal. When multiple sections were used per animal an appropriate distance between sections was allow to assure that a single synapse was not counted twice. Only micrographs which included at least one asymmetric synapse were included in the analysis. The total number of asymmetric synapses in each group was divided by the total area of tissue examined and expressed as the number of synapses/100 μm^2. Specificity of the biocytin labelling was assured by incubating tissue not exposed to biocytin in the avidin–biotin–peroxidase complex followed by DAB. No labelling was noted in these controls. Group means for the density of synapses was compared by a one-way ANOVA followed by a *post hoc* comparison (Fisher's PLSD). All values are reported as mean ± S.E.M. Significance was declared at $P<0.05$ and P values which were less than 0.01 were reported as $P<0.01$.

RESULTS

Density of unlabelled asymmetric synapses

The density of asymmetric synapses ($n=284$, where "n" refers to number of synapses from 118 micrographs) was compared among adult ($n=86$), P21 ($n=82$), P15 ($n=85$) and P10 ($n=31$) rats. Analysis of variance revealed a significant age-dependent increase in the density of asymmetric synapses ($F=8.0$, d.f.=3, 113, $P<0.01$). *Post hoc* tests revealed that the density of asymmetric synapses was significantly greater in adults (28.0 ± 3.5 synapses/100 μm^2), than at P15 (14.4 ± 1.3 synapses/100 μm^2) or P10 (11.5 ± 1.5 synapses/100 μm^2; $P<0.01$ for each comparison). At P21, the total density of asymmetric

Table 1. Density of asymmetric synapses from adult and neonatal rat neostriatum

	Age			
	Adult	P21	P15	P10
Total density of asymmetric synapses	28.0 (3.5)	24.2 (2.1)	14.4* (1.3)	11.5* (1.5)
Density of axodendritic synapses	3.9 (1.1)	6.0 (1.2)	5.7 (0.8)	7.2 (1.3)
Density of axospinous synapses	22.3 (3.0)	15.3* (1.8)	5.9* (1.1)	2.0* (0.7)

All values are the number of synapses/100 μm^2 ($\pm$S.E.M.)
Note that the total synaptic density and density of axospinous synapses at P15 and P10 are significantly lower than in adults while only axospinous values are significantly lower at P21. Values noted with (*) are significantly different from adult at $P<0.01$. There were no significant differences among neonates and adults for axodendritic synapses. It should be kept in mind that non-bias stereological techniques were not used therefore these values are used for comparisons and are not absolute values (see Discussion).

synapses (24.2 ± 2.1 synapses/100 μm^2) was not significantly different from that in adults (Table 1). The greatest increase in the density of asymmetric synapses occurred during the third postnatal week, between P15 and P21 (Table 1). It should be kept in mind that non-biased stereological techniques were not used, therefore the values for density of asymmetric synapses are intended for comparison purposes and are not absolute values (see Discussion). Figure 1 demonstrates the differences noted between adult and neonatal (P15) neostriatum. In the adult (Fig. 1A) asymmetric synapses are typically axospinous and are significantly more numerous than in the neonate (Fig. 1B) in which most asymmetric synapses form axodendritic synapses.

Density of axospinous synapses

The increased density of asymmetric synapses in the adult neostriatum appeared to be due primarily to an increase in the density of axospinous synapses. The synaptic input onto spine heads increased significantly in an age related manner ($F=33.3$, d.f. $=3,113$. $P<0.01$). The density of axospinous synapses was significantly greater in adults (22.3 ± 3.0 synapses/100 μm^2) than at all other ages: P21 (15.3 ± 1.8 synapses/100 μm^2), P15 (5.9 ± 1.1 synapses/100 μm^2) and P10 (2.0 ± 0.7 synapses/100 μm^2; $P<0.01$ for all comparisons) (Table 1).

Density of axodendritic synapses

In marked contrast to axospinous synapses, the density of asymmetric synapses terminating on dendritic shafts did not differ significantly among adults (3.9 ± 1.1 synapses/100 μm^2), P21 (6.0 ± 1.2 synapses/100 μm^2), P15 (5.7 ± 0.8 synapses/100 μm^2) or P10 (7.2 ± 1.3 synapses/100 μm^2) neonatal rats (Table 1).

Postsynaptic targets of unlabelled asymmetric synapses

The ratio of asymmetric axospinous or axodendritic synapses to the total number of asymmetric synapses (relative synaptic organization) showed a similar developmental pattern to that of synaptic density (Fig. 3). Axodendritic synapses comprised 7% of the asymmetric adult synapses in the neostriatum while comprising 13%, 41% and 67% in the P21, P15 and P10 neostriatum, respectively (Figs 2B, 3A). Axospinous synapses, however, comprised 89% of the adult asymmetric synapses and 82%, 57% and 30% at P21, P15, and P10, respectively (Fig. 3A). The postsynaptic target of the remaining synaptic profiles were unidentifiable.

Anterograde labelling of corticostriatal fibres

Biocytin-labelled terminals were identified on semi-serial sections (three to five sections). All labelled corticostriatal synaptic profiles formed asymmetric membrane specializations. Corticostriatal fibres most often terminated on spine heads (87%) in adults (Figs 2A, 3B). In the cases when biocytin-labelled fibres did not terminate on clearly-identified spine heads, these labelled fibres either ended on dendritic shafts (Fig. 1B), on the necks of dendritic spines or on unidentified postsynaptic targets. The proportion of labelled corticostriatal fibres terminating on spine heads showed an age-dependent relationship similar to that noted for unlabelled asymmetric synapses. P21 labelled terminals were very similar to adult synaptic profiles, with 83% of the labelled synapses forming axospinous contacts (Fig. 3B). The remaining targets were either axodendritic or unidentifiable. The axospinous synapses at P21 (Fig. 4A–C) are well defined similar to that noted in adults (Figs 1A, 2A) contrasted by axospinous synapses noted in the P15 (Fig. 5) and P10 (Figs 2B, 7) neonatal neostriatum.

Labelled corticostriatal terminals in P21 animals showed a very different organization than in the P15 animals as demonstrated in Figs 4 and 1B, respectively. At P15, the labelled terminals were generally located on dendritic shafts (43%). However, in P15 and P10 animals several labelled terminals were noted on spine heads, immature spine heads, and spine necks of immature spines (Figs 5A, B, 7). Immature spines (Figs 5A, B, 7) can be distinguished

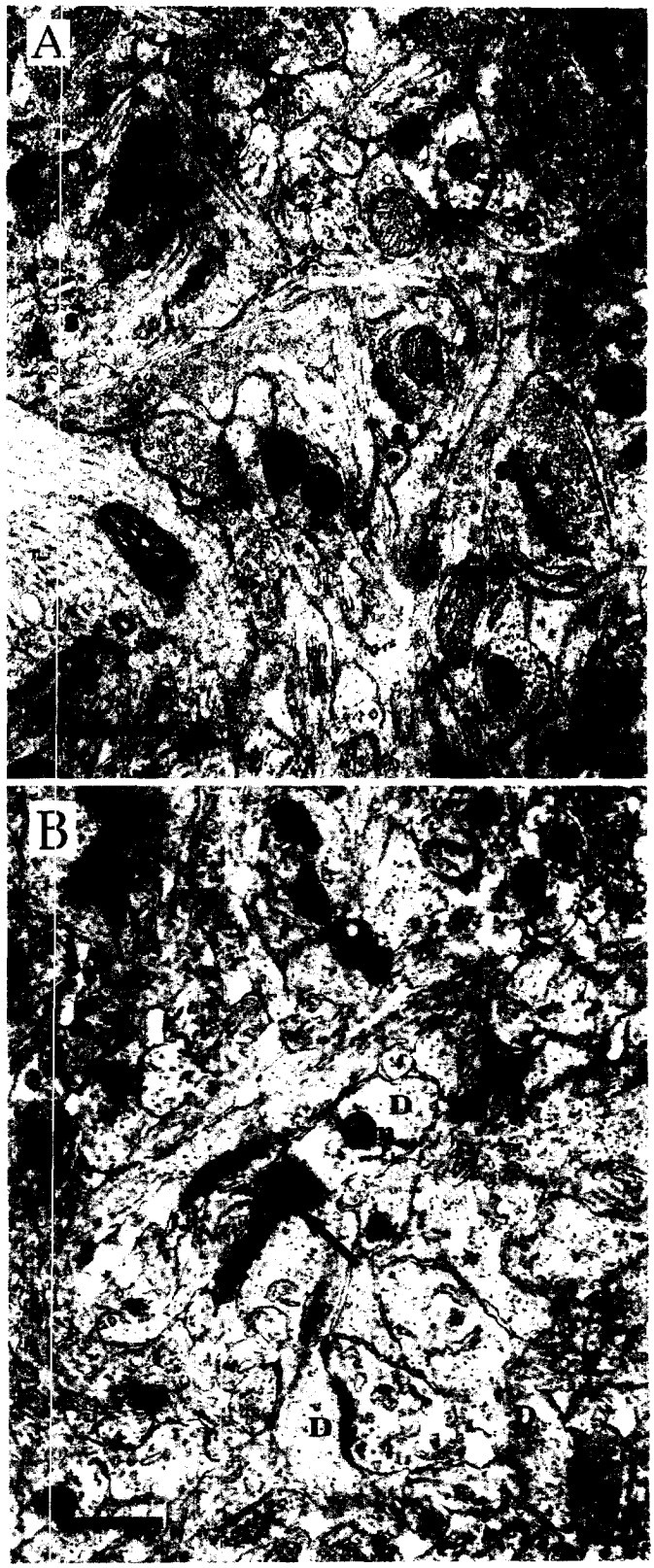

Fig. 1. Representative electron micrographs of comparable areas in the adult and P15 neostriatum. Each micrograph represents approximately 14 μm^2 of area. Note the relatively high density of asymmetric synapses in the adult (A) in comparison to P15 (B). In (A) all asymmetric synapses are onto spine heads (s). Note the well defined and mature spine apparatus (arrows). In (B) note that the three synapses are onto dendrites (D). Note the biocytin-labelled corticostriatal synaptic profile (arrow) terminating onto a dendrite (D) containing a mitochondrion (m). Scale bars = 0.5 μm.

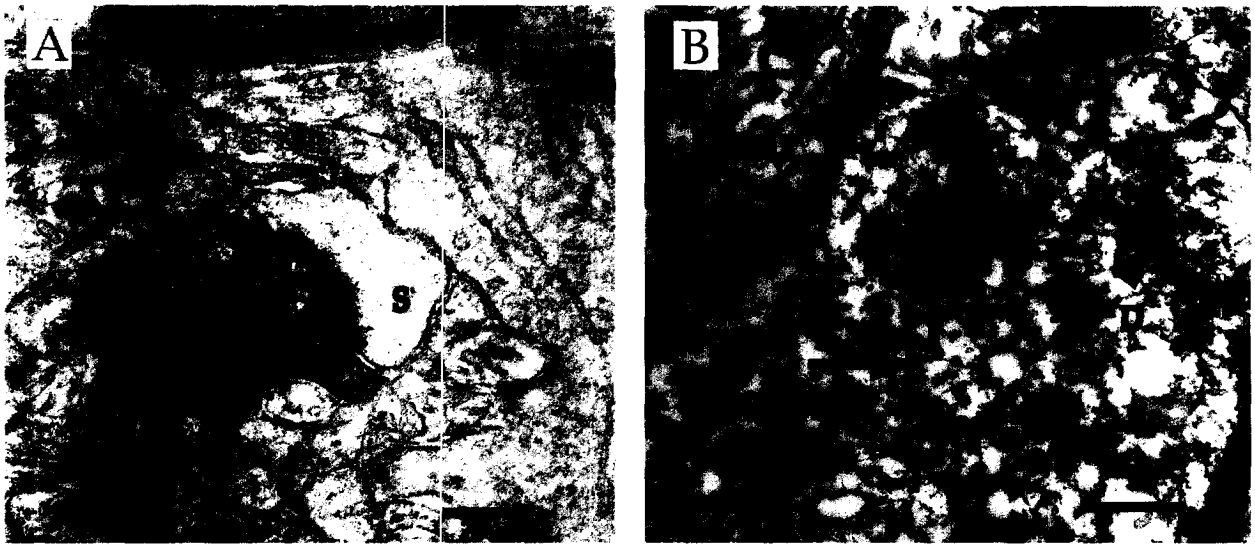

Fig. 2. Electron micrographs from an adult rat (A) and a P10 rat (B). In (A) a typical biocytin-labelled corticostriatal synaptic profile (arrow) terminates on a dendritic spine (s). Note the densely packed small round synaptic vesicles in the presynaptic synaptic profile. In (B) two synaptic profiles form asymmetric synapses (arrow heads) onto a single dendrite (D). Note the relatively loose packing of synaptic vesicles in the presynaptic terminal and the two mitochondria (m) and microtubules (arrow) in the postsynaptic dendrite. In addition, an asymmetric synapse (*) onto another dendrite is also present. Scale bars = 0.25 μm.

from mature spines (Figs 1A, 2A) by the presence of microtubule fragments and/or relatively large round vacuoles.[49] These large round vacuoles (considered to be immature spine apparatus) and microtubule fragments noted in dendritic spines at P15 and P10 were never noted in the P21 or adult neostriatum. In addition, the frequency of biocytin-labelled corticostriatal terminals was much lower in the younger neonates resulting in only a few labelled synapses being located in P10 and P15 animals.

Synaptic profile characteristics

Boutons at P21 appeared to be well organized and fully mature based on the number of synaptic vesicles per synaptic profile, length of the active zone, the ratio of vesicles per μm^2 of synaptic profile and total synaptic profile area (Fig. 6). Mean synaptic profile area during development decreased in an age related manner ($F=10.4$, d.f.$=3,164$, $P<0.01$) between P10 and adult. The synaptic profile area at P10 ($0.523 \pm .096\ \mu m^2$) was significantly greater compared to adult ($0.249 \pm .020\ \mu m^2$, $P<0.01$) (Fig. 6A) but similar among adult, P21 and P15. In order to establish whether the larger P10 synaptic profiles were the result of an age-dependent tissue swelling during processing, the mitochondrial cross-sectional area was measured and compared over development. This evaluation revealed an age-related increase in mean mitochondrial cross-sectional area ($F=7.4$, d.f.$=3,156$, $P<0.01$). Little difference was noted between P10, P15 and P21. In contrast, adult mitochondria ($0.044 \pm .003\ \mu m^2$) were significantly larger than P21, P15 and P10 mitochondria (0.029 to $0.033 \pm .002\ \mu m^2$, $P<0.01$ for all comparisons). These data suggest that tissue swelling was not responsible for the increase in synaptic profile area noted at P10.

The number of synaptic vesicles per synaptic profile showed an age-related increase between adult and P15 for total asymmetric synapses and for axospinous asymmetric synapses ($F=3.3$, d.f.$=3,202$, $P<0.05$ and $F=3.2$, d.f.$=3,146$, $P<0.05$, respectively) but not for asymmetric axodendritic synapses alone. The numbers of synaptic vesicles per synaptic profile for all asymmetric synapses combined and for axospinous asymmetric synapses were significantly greater in adults (40.1 ± 2.9 and 40.7 ± 3.0 vesicles/synaptic profile, respectively) compared to P15 (28.6 ± 2.5 and 27.1 ± 3.2 vesicles/synaptic profile, respectively; $P<0.01$) (Fig. 6C). The number of vesicles per asymmetric synaptic profile at P21 and P10 were not different from that noted in adults. However, when the density of synaptic vesicles per μm^2 of synaptic profile was compared over development, an age-related increase was noted ($F=3.8$, d.f.$=3,256$, $P<0.01$) (Figs 6B, 7). The density of vesicles was significantly greater in adult (191.9 ± 8.4 vesicles/μm^2 area of synaptic profile) compared to P10 (130.8 ± 21.3 vesicles/μm^2 area of synaptic profile, $P<0.01$) (Figs 6B, 7). Figure 7 demonstrates the relatively loose packing of synaptic vesicles when compared to the adult neostriatum (Figs 1A, 2B).

The length of the active zone for asymmetric axospinous synapses increased slightly over development, in an age related manner ($F=2.6$, d.f.$=3,172$,

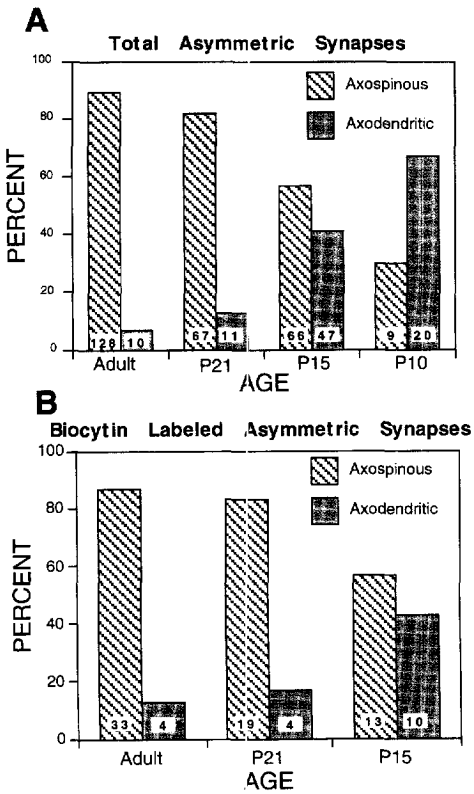

Fig. 3. Postsynaptic termination sites of total relative asymmetric (A) and biocytin-labelled corticostriatal asymmetric (B) synapses in the adult and neonatal neostriatum as a function of age. In (A) note the high proportion of axospinous synapses in the adult and P21 rats. In (B) the proportion of biocytin-labelled corticostriatal axodendritic synapses is low in adults and P21 rats and shows a large increase in the P15 rats (insufficient number of biocytin-labelled corticostriatal terminals were noted for P10 rats to be included in this comparison). Approximately half of the P15 axospinous synapses were on immature spines (see text).

$P=0.053$) (Fig. 6D). Axospinous active zone length in adults (319.0 ± 13.1 μm) was significantly greater than that at P21 (268.8 ± 15.0 μm, $P=0.05$) and P15 (275.6 ± 15.0 μm, $P<0.05$). P10 active zone length was slightly but not significantly greater than in adults. This appears to be the result of the P10 synaptic profiles generally being larger in size and the low number of axospinous synapses noted at P10. Active zone length for axodendritic synapses were similar at all ages evaluated.

DISCUSSION

Density of synapses

Approximately 95% of the cells of the neostriatum are medium spiny neurons.[16] The size and shape of the neostriatal medium spiny neuron is similar in adult and neonatal rats[43–45] and by the age evaluated in this study, the number of cells in the neonatal and adult neostriatum are equal.[2,14,31,32] One of the concerns of reporting synaptic density data is that bias may result due to changes in bouton size or the total volume of the neostriatum that may occur during development.[8,9,42,48] An increase in bouton size over development could result in a greater number of profiles being counted per bouton in older neostriatum.[8,9,42,48] Additionally, if the volume of the neostriatum decreased over development the total number of boutons could remain constant but appear to increase due to the same number of synapses being compressed into a smaller area. Neither of these two concerns appears likely. Our data show that the measured area of P10 synaptic profiles was significantly greater than adults which strongly argues against changes in bouton size accounting for the observed developmental differences since larger boutons would result in a greater number of synaptic profiles being detected and counted in the neonate compared to adult. Therefore these data actually suggest that the developmental differences in our density data may be underestimated.[8,9,42,48] Additionally, previous work of Fentress *et al.*[14] and Fisher *et al.*[15] has shown that the volume of the neostriatum in rats and felines significantly increases over development. Since neostriatal volume increases over development, if the number of synapses remained constant the density of synapses would decrease over development. Again, these data actually suggest that the developmental differences in our density data may be underestimated. With this said, it should be kept in mind that non-biased stereological techniques were not used therefore the synaptic density values reported must be considered as estimates used for comparisons and not as absolute values.

In the present study, the synaptic connectivity of the developing rat neostriatum was observed to change significantly during the first three postnatal weeks. The increase in the density of asymmetric synapses noted during development can be attributed primarily to the development of axospinous synaptic terminals since the density of axodendritic synapses remained relatively constant at all ages evaluated. The density of terminals forming asymmetric synapses ending on spine heads showed a significant increase during postnatal development. Similar results have been noted in the feline and primate neostriatum.[1,11] The largest increase in the total density of asymmetric and axospinous synapses occurred during the third postnatal week, between P15 and P21. This time period is in good agreement with previous morphological studies in which neonatal medium spiny neurons were intracellularly labelled *in vivo* with biocytin.[43,44] The medium spiny neuron appears generally aspiny, with thin and varicose dendrites prior to the third postnatal week.[45] During the third postnatal week, as dendritic spine density increases, medium spiny neurons begin to take on their typical spiny appearance. The finding of increased synaptic density in this study is also consistent with the previous finding that the majority of

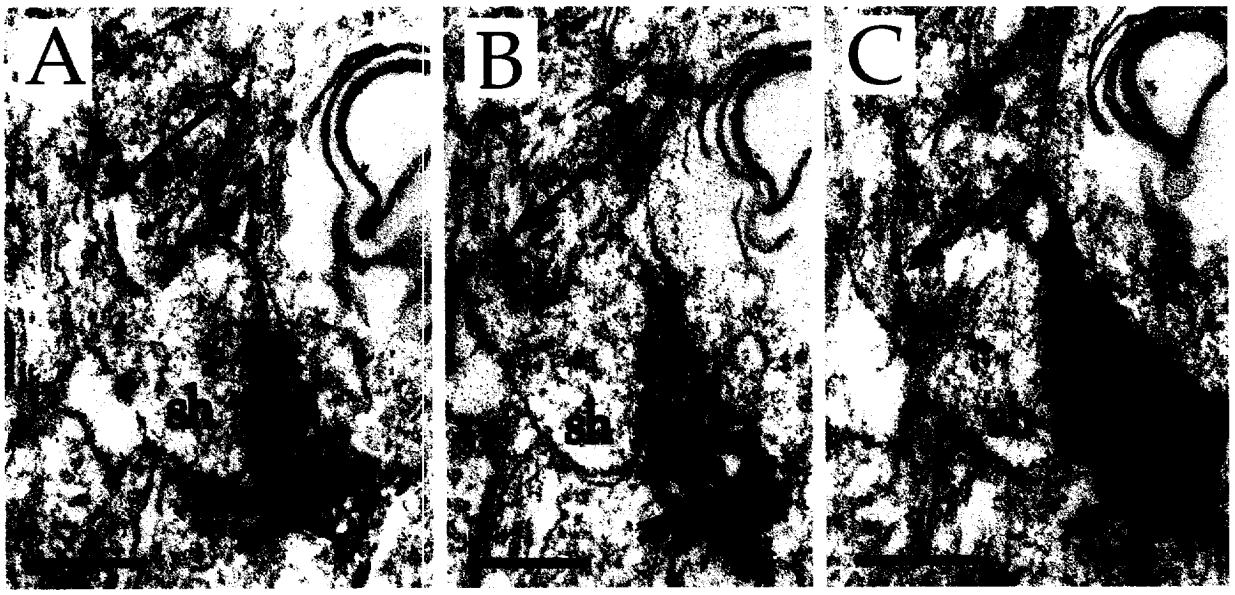

Fig. 4. Electron micrographs of a single biocytin-labelled corticostriatal terminal from a P21 rat in consecutive serial sections (A, B and C). Note that as in adults (see Figs 1 and 2) at P21 corticostriatal afferents typically terminate onto the heads of dendritic spines. In all three micrographs the biocytin-labelled corticostriatal input (arrowhead) terminates onto a well-defined mature spine head (sh). The spine neck (arrow) for this dendritic spine can be clearly seen. This is substantially different from what is noted at P15 and P10 (see Figs 1, 2 and 7) indicating that by the end of the third postnatal week cortical inputs have reached a certain level of maturity. Scale bars=0.25 μm.

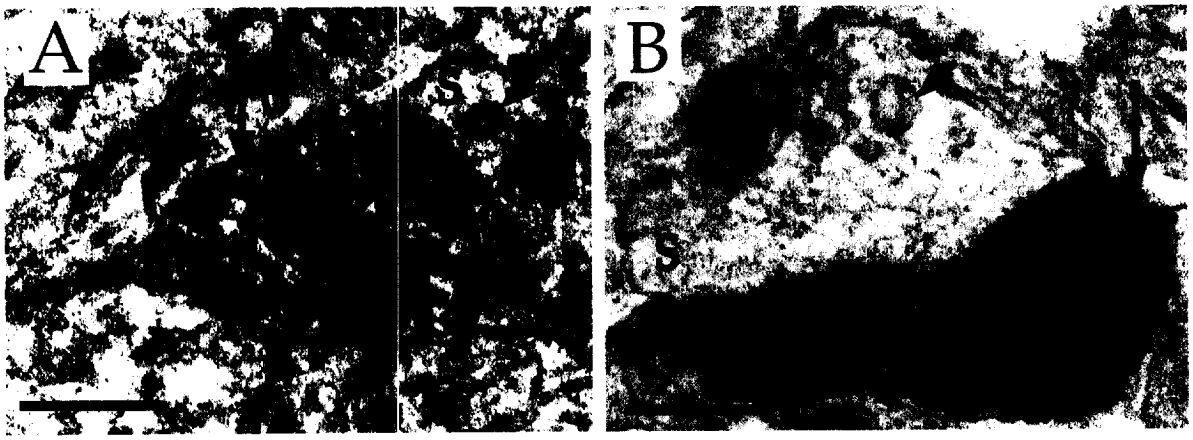

Fig. 5. Electron micrographs of biocytin-labelled corticostriatal terminals in P15 rats. In (A) note the biocytin-labelled corticostriatal afferent (arrow) terminating on an immature spine (s). The spine contains a relatively large vacuole (arrowhead) which has been associated with immature spine apparatus and therefore dendritic spines.[49] Also present is an apposition with an additional structure (*). In (B) a biocytin-labelled (arrow) profile terminates onto an immature spine head (s). The spine head is considered immature due to the presence of a large round vacuole similar to that noted in A (arrowhead).[49] Scale bars=0.25 μm.

the cortical and thalamic afferents innervate the neostriatum during the third postnatal week.[19]

Relative synaptic organization

The proportion of axodendritic synapses decreases over development while the density of axodendritic synapses remains relatively constant. The changes noted in the proportion of axodendritic synapses is contrasted by the total density of asymmetric synapses which increases significantly over development. These data show that the decrease in the proportion of asymmetric axodendritic synapses is not the result of a decrease in the number of axodendritic boutons during development, but is the result of a higher density of asymmetric synapses in the adult neostriatum. The higher density of asymmetric synapses in the adult is primarily due to a large increase in the

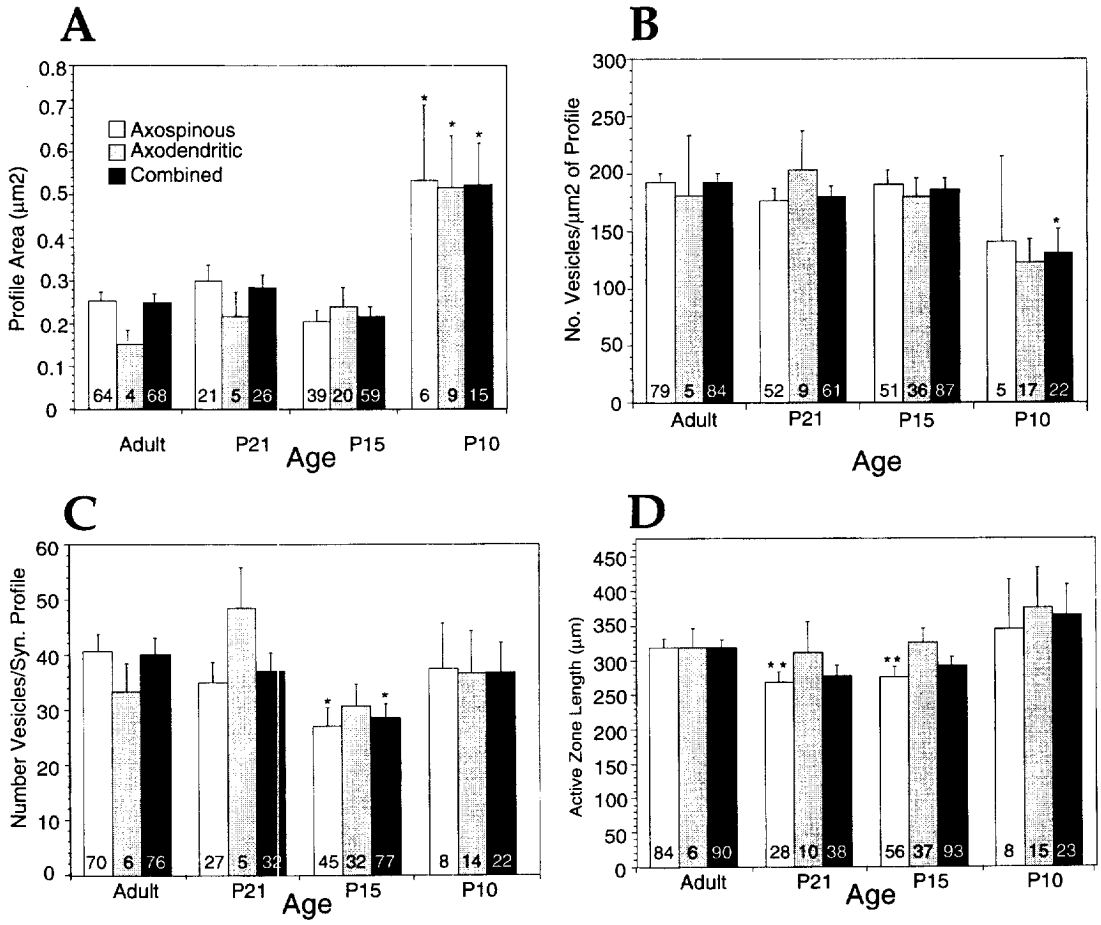

Fig. 6. The synaptic profile area (A), the relative synaptic vesicle density (B, number of synaptic vesicles per mm^2 of synaptic profile area), number of vesicles per synaptic profile (C) and the active zone length (D) compared over development. In (A) note that synaptic profile size at P10 is significantly greater than in adults for axospinous, axodendritic and combined axospinous/axodendritic asymmetric synaptic specializations. In (B) note that the relative density of synaptic vesicles in adults is significantly greater than the combined P10 axospinous/axodendritic asymmetric synaptic specializations. It appears that the relative density of synaptic vesicles for axospinous and axodendritic synaptic specializations was not significantly different from adult due to a low "n" and high degree of variability at P10. In (C) note that the number of vesicles per synaptic profile was significantly less at P15 for axospinous and axospinous/axodendritic asymmetric synaptic specializations but not axodendritic synapses. In (D) note that the active zone length is significantly shorter compared to adult for axospinous asymmetric synaptic specializations for P21 and P15 while axodendritic active zone length appears to change little over development ($*P<0.01$, $**P\leq 0.05$).

density of asymmetric axospinous synapses with little change in the density of axodendritic synapses. These findings are consistent with previous findings in the primate, in which the relative proportion of neostriatal axospinous synapses also increased over development.[11] The origin of the asymmetric axodendritic synapses as corticostriatal or thalamostriatal was not determined in this study. However, it should be noted that a large proportion of asymmetric axodendritic synapses in adults are known to be mostly thalamic in origin.[38] Even though in the feline corticostriatal and thalamostriatal afferents appear to be equally present during postnatal development,[15] it may be the case that in the neonatal rat thalamostriatal axodendritic synapses appear relatively early in postnatal development and are thus disproportionately distributed. Regardless of the origin of excitatory inputs, by P21 the relative proportions of axodendritic and axospinous synapses are similar to that in adults. This suggests that excitatory synaptic input to the neostriatum is almost fully established by P21, suggesting that by P21, the neostriatum and medium spiny neuron should begin to display adult-like functional properties (see functional considerations below).

Biocytin-labelled afferents

Most of the labelled corticostriatal afferents in neonates prior to P21 terminated on dendritic shafts or immature spines. This is in contrast to what was noted in older animals, where the majority of labelled

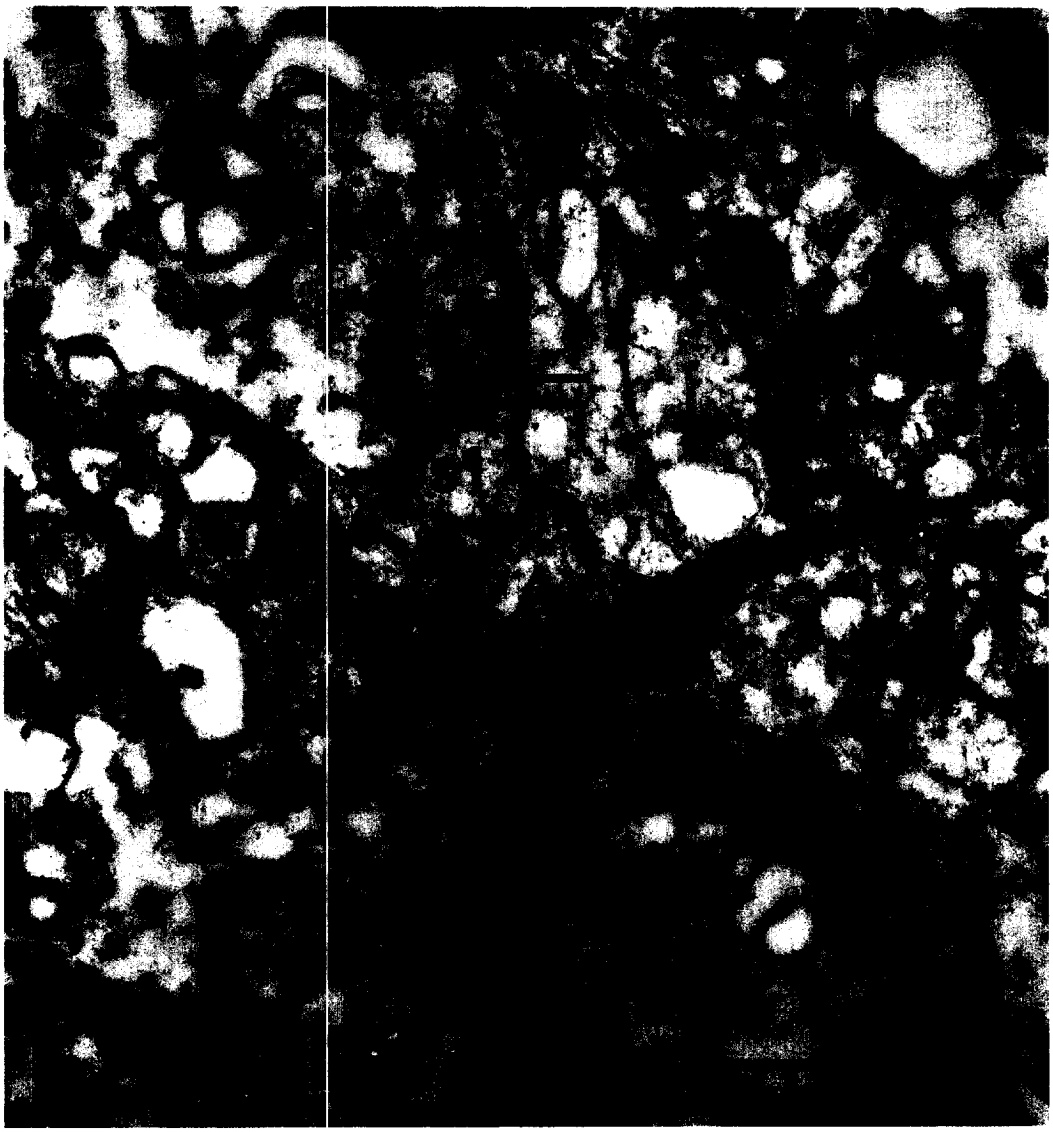

Fig. 7. Electron micrograph showing two asymmetric axospinous synapses in the P10 neostriatum. Both spines (s1 and s2) are immature and contain relatively large segments of microtubules (arrowheads) as well as large round vacuoles considered to be immature spine apparatus (double arrows).[49] The microtubule in one spine (s2) appears to be embedded into an electron-dense vacuole. In the presynaptic terminals the synaptic vesicles are relatively loosely arranged (*) with one presynaptic terminal containing what appears to be a large dense core vesicle (arrow). Scale bar=0.5 μm.

corticostriatal fibres terminated on spine heads as previously reported.[10,24–26,28,41] These data are also consistent with both the synaptic density and general synaptic organization, suggesting that the adult configuration of corticostriatal excitatory afferents has been established by P21.

Synaptic profile characteristics

The increase in the number of vesicles per synaptic profile, the ratio of vesicles/μm^2 of synaptic profile and active zone length over development, considered with the above discussed data, suggest that excitatory asymmetric synapses are functionally immature prior to P21.[36] Of particular interest is that the active zone length at P21 and P15 is significantly smaller when compared to adult for axospinous asymmetric synapses but not for axodendritic synapses. These findings are consistent with developmental studies of the primate neostriatum in which active zone length was also noted to increase over postnatal development.[12] Taken together, these data may indicate that axodendritic synapses are more functionally mature than existing axospinous synapses in neonates.[36] This conclusion is supported by the observation that the density of axodendritic synapses remains constant over development, suggesting that these synapses are established earlier in the development of the neostriatum.

Functional considerations

Morphological establishment of the excitatory inputs to the medium spiny neuron does not necessarily indicate that these connections are fully functional. The typical electrophysiological characteristics of adult spiny neurons consisting of the cortically-evoked excitatory postsynaptic potential (EPSP)/long-lasting hyperpolarization/depolarization,[4,6,20,51] up and down states[53] and the irregular and bursty spontaneous activity,[10] do not begin to become evident prior to postnatal week 3.[43] Cortical stimulation in the neonate results in a simple EPSP.[33,43,44] The mean maximal EPSP amplitude does not change over development even though the number of excitatory inputs increases significantly.[19,43,44] The present study showed that in the neonate the principal excitatory input to the neostriatum terminates onto dendritic shafts while in the adult neostriatum the vast majority of excitatory input terminates onto spine heads. This change in the termination sites of the newly arriving excitatory inputs may help to explain why mean maximal EPSP amplitude remains constant over development while the overall level of excitatory input increases. Prior to spine formation the medium spiny neuron is significantly more electrotonically compact compared to adults.[50,52] Therefore, in neonates each individual excitatory axodendritic synapse has the capability of more strongly influencing the membrane potential of the medium spiny neuron than is the case in the adult. The arrival of the massive excitatory input and the formation of dendritic spines and axospinous synapses, increases the electrotonic length of the spiny neuron significantly.[50] Thus, each individual excitatory input is attenuated by the dendritic spines and contributes less to the overall membrane potential of the medium spiny neuron. The mean maximal EPSP amplitude of the medium spiny neuron may therefore remain constant over development despite the increase in the number of excitatory synapses because the synaptic "weight" of the axospinous synapses is less than that of the axodendritic synapses and the electrotonic length of the neuron increases with spine development.

Spontaneous activity is essentially absent in the rat neostriatum prior to P15.[34,43] Despite the fact that stimulation of the cortex is able to excite the medium spiny neuron both in the neonate and in the adult, there are significantly fewer excitatory synapses in the neonatal neostriatum. These data may help explain the lack of spontaneous activity in the neostriatum. Spontaneous activity can also be affected by intrinsic and/or feedforward inhibition since the reduced density and/or activity of excitatory inputs might unmask intrinsic inhibitory properties of the striatum that are difficult to observe in adults. This unmasking may be the result of inhibitory synapses being relatively well developed prior to P10.[40] In addition, while passing through the neonatal cortex, *en route* to the neostriatum, little activity has been noted, suggesting a low level of spontaneous activity in the cortex.[43] Also the cortical afferents which are present may not be fully mature, as demonstrated by the significantly larger synaptic profile size and reduced vesicle density at P10.

Long-lasting hyperpolarization in neostriatal neurons following the initial EPSP-elicited by cortical or thalamic stimulation has been hypothesized as being the result of disfacilitation of corticostriatal or thalamostriatal afferents[51] and not from feedback or feedforward inhibition. Additionally, Wilson *et al.*,[53] argue that the discrete up and down states of membrane potential noted in the adult spiny neuron *in vivo* result from an interaction of correlated excitatory afferent input and intrinsic membrane properties. The results of the current study lend support to this conclusion since many of the mature excitatory axospinous terminals are established between P15 and P21, the same period when long-lasting hyperpolarization and up and down states first become apparent.[43] If the long-lasting hyperpolarization and up and down states resulted from intrinsic inhibitory synaptic mechanisms one would expect these properties to be apparent early in development, because prior to postnatal week 3, the axon collateral plexus, inhibitory synapses and intrinsic GABAergic neurons are well developed[2,14,22,40,43,45] and medium spiny neurons are responsive to application of GABA agonists.[29] However, this is not the case.[43,44] Since the long-lasting hyperpolarization and up and down states only begin to become apparent during postnatal week 3, the results of this study support the idea that these phenomena are relatively independent of intrinsic inhibitory synaptic connections.

Prior to the third postnatal week, cortical stimulation can result in an inhibitory postsynaptic potential (IPSP) which is not seen in the adult neostriatum.[43] The fact that IPSPs can be more easily demonstrated in the neonatal neostriatum than in the adult may be due to the relatively low density of asymmetric excitatory synapses. The effects of feedforward or feedback inhibition on medium spiny neurons receiving relatively few excitatory boutons would be far more apparent than in the adult striatum.[43] Additionally, some of the asymmetric axodendritic synapses noted over development almost certainly terminate onto dendritic shafts of intrinsic neurons, including the parvalbumin GABAergic neurons. Corticostriatal afferents, in the adult rat and monkey, are known to form axodendritic synapses with parvalbumin immunoreactive postsynaptic targets[3,28] which are known to make synaptic contracts with medium spiny neurons.[3,27] Since the density of axodendritic synapses remains constant over development, these data suggest that the postsynaptic target of a portion of the axodendritic synapses noted in this study may be parvalbumin interneurons which might play a role in the cortically evoked IPSP

noted in neonates.[27] In support of this, simultaneous whole-cell recordings from parvalbumin-containing interneurons and medium spiny neurons have demonstrated that parvalbumin interneurons are in monosynaptic contact with medium spiny neurons as early as P16. Stimulation of single parvalbumin interneurons produce large IPSPs in medium spiny neurons. The IPSP amplitude is substantially larger in slices from early neonates compared to those slices taken from pups after the third postnatal week.[23a] Taken together with these data present above would suggest that the IPSP is more apparent in the neonate due to fewer excitatory inputs being present and the strong influence of parvalbumin interneurons on the medium spiny neuron prior to P20.

The absence of the long-lasting hyperpolarization and up and down states, the presence of IPSPs and a lower spine density are not only characteristics of the neonatal striatum but are also characteristics shared by medium spiny neurons in grafts of fetal neostriatum.[43,47,55,56] The present study shows a similar pattern of synaptic connectivity for the neonatal striatum as has been noted in fetal neostriatal neurons grafted to ibotenic or kainic acid treated neostriatum.[13,54] Both the neonatal neostriatum and fetal grafts have a decreased density of asymmetric axospinous synapses with an increased proportion of axodendritic terminals when compared to adults or host striatum, respectively. This suggest that the absence of the long-lasting hyperpolarization following the cortically evoked EPSP and the IPSP seen in neonatal neostriatal neurons *in situ* as well as in grafted neostriatal neurons may derive from a relative paucity of functional cortical afferents.

CONCLUSION

The anatomical establishment of excitatory axospinous inputs to medium spiny neurons in the neostriatum corresponds to and helps explain functional changes noted over development in the electrophysiology of the medium spiny neuron. These findings allow for a greater understanding of the functional role excitatory afferents play in both the neonatal and adult neostriatum.

Acknowledgements—Supported by NS 30679 and NS 34865. We would like to thank L. Zaborszky and T.Z. Koós for their helpful comments and advice and Schering–Plough Research Institute for the use of their electron microscopy facilities.

REFERENCES

1. Adinolfi A. (1977) The postnatal development of the caudate nucleus: a Golgi and electron microscopic study of kittens. *Brain Res.* **133,** 251–266.
2. Bayer S. A. (1984) Neurogenesis in the rat neostriatum. *Int. J. dev. Neurosci.* **2,** 163–175.
3. Bennett B. D. and Bolam J. P. (1994) Synaptic input and output of parvalbumin-immunoreactive neurons in the neostriatum of the rat. *Neuroscience* **62,** 707–719.
4. Buchwald N. A., Price D. D., Vernon L. and Hull C. D. (1973) Caudate intracellular responses to thalamic and cortical inputs. *Expl Neurol.* **38,** 311–323.
5. Calabresi P., Mercuri N. B., Stefani A. and Bernardi G. (1990) Synaptic and intrinsic control of membrane excitability of neostriatal neurons. I. An *in vivo* analysis. *J. Neurophysiol.* **63,** 651–662.
6. Calabresi P., Pisani A., Mercuri N. B. and Bernardi G. (1996) The corticostriatal projection: from synaptic plasticity to dysfunctions of the basal ganglia. *Trends Neurosci.* **19,** 19–24.
7. Cepeda C., Walsh J. P., Buchwald N. A. and Levine M. S. (1991) Neurophysiological maturation of cat caudate neurons: evidence from *in vitro* studies. *Synapse* **7,** 278–290.
8. Coggeshall R. E. (1992) A consideration of neural counting methods. *Trends Neurosci.* **15,** 9–13.
9. Coggeshall R. E. and Lekan H. A. (1996) Methods for determining numbers of cells and synapses: a case for more uniform standards of review. *J. comp. Neurol.* **364,** 6–15.
10. Cowan R. L. and Wilson C. J. (1994) Spontaneous firing patterns and axonal projections of single corticostriatal neurons in the rat medial agranular cortex. *J. Neurophysiol.* **71,** 17–32.
11. DiFiglia M., Pasik T. and Pasik P. (1976) Quantitative morphology of monkey neostriatum: one-week old vs adult. *Soc. Neurosci. Abstr.* **2,** 61.
12. DiFiglia M., Pasik P. and Pasik T. (1980) Early postnatal development of the monkey neostriatum: a Golgi and ultrastructural study. *J. comp. Neurol.* **190,** 303–331.
13. DiFiglia M., Schiff L. and Deckel A. W. (1988) Neuronal organization of fetal striatal grafts in kainate- and sham-lesioned rat caudate nucleus: light- and electron-microscopic observations. *J. Neurosci.* **8,** 1112–1130.
14. Fentress J. C., Stanfield B. B., Cowan W. M. (1981) Observations on the development of the striatum in mice and rats. *Anat. Embryol.* **163,** 275–298.
15. Fisher R. S., Levine M. S., Gazzara R. A., Hull C. D. and Buchwald N. A. (1983) Postnatal development of caudate input neurons in the cat. *J. comp. Neurol.* **219,** 51–69.
16. Graveland G. A. and DiFiglia M. (1985) The frequency and distribution of medium-sized neurons with indented nuclei in the primate and rodent neostriatum. *Brain Res.* **327,** 308–311.
17. Graybiel A. M. and Ragsdale C. W. (1979) Fiber connections of the basal ganglia. *Prog. Brain Res.* **51,** 239–283.
18. Graybiel A. M. and Ragsdale C. W. (1983) Biochemical anatomy of the striatum. In *Chemical Neuroanatomy* (ed. Emson P. C.), pp. 427–504. Raven, New York.
19. Hattori T. and McGeer P. L. (1973) Synaptogenesis in the corpus striatum of infant rat. *Expl Neurol.* **38,** 70–79.

20. Herrling P. L. (1984) Evidence for GABA as the transmitter for early cortically evoked inhibition of cat caudate neurons. *Expl Brain Res.* **55,** 528–534.
21. Hull C. D., McAllister J. P., Levine M. S. and Adinolfi A. M. (1981) Quantitative developmental studies of feline neostriatal spiny neurons. *Devl Brain Res.* **1,** 309–332.
22. Hwang B. H. and Hoovler D. W. (1982) Characterization of monoaminergic terminals in the neostriatum of neonatal rats: an electron microscopic morphometric analysis. *Devl. Brain Res.* **5,** 104–107.
23a. Johnson L., Koós T., Zaborszky L., Moore K. and Tepper J. M. (1997) $GABA_A$ receptor-mediated inhibition of medium spiny neurons by fast spiking interneurons in rat neostriatum. *Soc. Neurosci. Abstr.* **23,** 1279.
23b. Jones E. G. and Leavitt R. Y. (1974) Retrograde axonal transport and the demonstration of nonspecific projections to the cerebral cortex and striatum from the thalamic intralaminar nuclei in the rat, cat and monkey. *J. comp. Neurol.* **154,** 349–378.
24. Kemp J. M. and Powell T. P. S. (1971) The structure of the caudate nucleus of the cat: light and electron microscopy. *Phil. Trans. R. Soc.* **262,** 383–401.
25. Kemp J. M. and Powell T. P. S. (1971) The synaptic organization of the caudate nucleus. *Phil. Trans. R. Soc.* **262,** 403–412.
26. Kemp J. M. and Powell T. P. S. (1971) The site of termination of afferent fibers in the caudate nucleus. *Phil. Trans. R. Soc.* **262,** 413–427.
27. Kita H. (1993) GABAergic circuits of the striatum. In *Chemical Signaling in the Basal Ganglia* (eds Arbuthnott G. W. and Emson P. C.), Vol. 99, pp. 51–72. Elsevier, New York.
28. Lapper S. R., Smith Y., Sadikot A. F., Parent A. and Bolam J. P. (1992) Cortical input to parvalbumin-immunoreactive neurones in the putamen of the squirrel monkey. *Brain Res.* **580,** 215–224.
29. Levine M. S., Adams C. E., Hannigan J. H., Hull C. D. and Buchwald N. A. (1990) Caudate neurons respond to excitatory and inhibitory amino acids in early postnatal periods in the cat. *Devl Neurosci.* **12,** 196–203.
30. Levine M. S., Fisher R. S., Hull C. D. and Buchwald N. A. (1982) Development of spontaneous neuronal activity in the caudate nucleus, globus pallidus-entopeduncular nucleus, and substantia nigra of the cat. *Devl Brain Res.* **3,** 429–441.
31. Mahalik T. J. (1994) Programmed cell death in the striatum of the neonatal rat. *Soc. Neurosci. Abstr.* **20,** 688.
32. Mahalik T. J. and Altar C. A. (1996) Programmed cell death in the developing rat striatum and attenuation by BDNF but not NT-3. *Soc. Neurosci. Abstr.* **22,** 996.
33. Morris R., Levine M. S., Cherubini E., Buchwald N. A. and Hull C. D. (1979) Intracellular analysis of the development of responses of caudate neurons to stimulation of cortex, thalamus and substantia nigra in the kitten. *Brain Res.* **173,** 471–487.
34. Napier T. C., Coyle S. and Breese G. R. (1985) Ontogeny of striatal unit activity and effects of single or repeated haloperidol administration in rats. *Brain Res.* **333,** 35–44.
35. Paxinos G. and Watson C. (1986) *The Rat Brain in Stereotaxic Coordinates*. 2nd edn, Academic, San Diego.
36. Pierce J. P. and Lewin G. R. (1994) An ultrastructural size principle. *Neuroscience* **58,** 441–446.
37. Royce G. J. (1978) Cells of origin of subcortical afferents to the caudate nucleus: a horseradish peroxidase investigation in the cat. *Brain Res.* **146,** 145–150.
38. Sadikot A. F., Parent A., Smith Y. and Bolam J. P. (1992) Efferent connections of the centromedian and parafascicular thalamic nuclei in the squirrel monkey: a light and electron microscopic study of the thalamostriatal projection in relation to striatal heterogeneity. *J. comp. Neurol.* **320,** 228–242.
39. Sharpe N. A. and Tepper J. M. (1993) Development of the rat neostriatal synaptic neuropil. *Soc. Neurosci. Abstr.* **19,** 1434.
40. Sharpe N. A. and Tepper J. M. (1995) Development of inhibitory synapses in rat neostriatum. *Soc. Neurosci. Abstr.* **21,** 1424.
41. Sharpe N. A., Trent F. and Tepper J. M. (1992) Postnatal changes in neostriatal synaptic input. *Soc. Neurosci. Abstr.* **18,** 697.
42. Sterio D. C. (1984) The unbiased estimation of number and sizes of arbitrary particles using the disector. *J. Microsc.* **134,** 127–136.
43. Tepper J. M. and Trent F. (1993) *In vivo* studies of the postnatal development of rat neostriatal neurons. In *Chemical Signaling in the Basal Ganglia* (eds Arbuthnott G. W. and Emson P. C.), Vol. 99, pp. 35–50. Elsevier, New York.
44. Trent F. and Tepper J. M. (1991) Postnatal development of synaptic responses, membrane properties and morphology of rat neostriatal neurons *in vivo*. *Soc. Neurosci. Abstr.* **17,** 938.
45. Trent F. and Tepper J. M. (1993) Morphological development of rat neostriatal medium spiny neurons intracellularly labeled with biocytin. *Soc. Neurosci. Abstr.* **19,** 1434.
46. Veening J. G., Cornelissen F. M. and Lieven P. A. J. M. (1980) The topical organization of the afferents to the caudatoputamen of the rat. A horseradish peroxidase study. *Neuroscience* **5,** 1233–1268.
47. Walsh J. P., Zhou F. C., Hull C. D., Fisher F. S., Levine M. S. and Buchwald N. A. (1988) Physiological and morphological characterization of striatal neurons transplanted into the striatum of adult rats. *Synapse* **2,** 37–44.
48. West M. J. (1993) New stereological methods for counting neurons. *Neurobiol. Aging* **14,** 275–285.
49. Westrum L. E., Jones D. H., Gray E. G. and Barron J. (1980) Microtubules, dendritic spines and spine apparatuses. *Cell Tiss. Res.* **208,** 171–181.
50. Wilson C. J. (1984) Passive cable properties of dendritic spines and spiny neurons. *J. Neurosci.* **4,** 281–297.
51. Wilson C. J. (1986) Postsynaptic potentials evoked in spiny neostriatal projection neurons by stimulation of ipsilateral and contralateral neocortex. *Brain Res.* **367,** 201–213.
52. Wilson C. J., Groves P. M., Kitai S. T. and Linder J. C. (1983) Three-dimensional structure of dendritic spines in the rat neostriatum. *J. Neurosci.* **3,** 383–398.
53. Wilson C. J. and Kawaguchi Y. (1996) The origins of two-state spontaneous membrane potential fluctuations of neostriatal spiny neurons. *J. Neurosci.* **16,** 2397–2410.
54. Xu Z. C., Wilson C. J. and Emson P. C. (1989) Restoration of the corticostriatal projection in rat neostriatal grafts: electron microscopic analysis. *Neuroscience* **29,** 539–550.

55. Xu Z. C., Wilson C. J. and Emson P. C. (1991) Synaptic potentials evoked in spiny neurons in rat neostriatal grafts by cortical and thalamic stimulation. *J. Neurophysiol.* **65,** 477–493.
56. Zemanick M. C., Walker P. D. and McAllister J. P. II (1987) Quantitative analysis of dendrites from transplanted neostriatal neurons. *Brain Res.* **414,** 149–152.

(*Accepted* 29 *October* 1997)